Purinergic Signalling (2014) 10:619–629
DOI 10.1007/s11302-014-9424-5

ORIGINAL ARTICLE

PQ-69, a novel and selective adenosine A_1 receptor antagonist with inverse agonist activity

Min Lu · Bo Wang · Cheng Zhang · Xiaomei Zhuang · Mei Yuan · Haoshan Wang · Weizhang Li · Ruibin Su · Jin Li

Received: 15 June 2014 / Accepted: 18 August 2014 / Published online: 24 September 2014

Abstract Potent and selective adenosine A_1 receptor (A_1AR) antagonists with favourable pharmacokinetic properties used as novel diuretics and antihypertensives are desirable. Thus, we designed and synthesized a series of novel 4-alkylamino substitution-2-arylpyrazolo[4,3-c]quinolin-3-one derivatives. The aim of the present study is to characterize the biological profiles of the optimized compound, PQ-69. In vitro binding assay revealed a K_i value of 0.96 nM for PQ-69 in cloned hA_1 receptor, which was 217-fold more selective compared with hA_{2A} receptors and >1,000-fold selectivity for hA_1 over hA_3 receptor. The results obtained from [^{35}S]-GTPγS binding and cAMP concentration assays indicated that PQ-69 might be an A_1AR antagonist with inverse agonist activity. In addition, PQ-69 displayed highly inhibitory activities on isolated guinea pig contraction (pA2 value of 8.99) induced by an A_1AR agonist, 2-chloro-N6-cyclopentyl adenosine. Systemic administration of PQ-69 (0.03, 0.3, 3 mg/kg) increased urine flow and sodium excretion in normal rats. Furthermore, PQ-69 displayed better metabolic stability in vitro and longer terminal elimination half-life ($t_{1/2}$) in vivo compared with 1,3-dipropyl-8-cyclopentylxanthine. These findings suggest that PQ-69 exhibits potent antagonist effects on A_1AR in vitro, ex vivo and in vivo, it might be a useful research tool for investigating A_1AR function, and it could be developed as a potential therapeutic agent.

Keywords 4-butylamino-2-(3-fluorophenyl)[4,3-c]quinolin-3-one · Non-xanthine adenosine A_1 receptor (A_1AR) antagonist · Inverse agonism · Diuresis

Introduction

Adenosine is an important endogenous modulator with a large variety of physiological functions acting on four different adenosine receptor (AR) subtypes, named A_1, A_{2A}, A_{2B} and A_3. Upon activation, A_1 and A_3 AR may inhibit adenylyl cyclase, which results in a decrease in cyclic AMP level and stimulates phospholipase C and phospholipase D via $G_{i/o}$ protein, whereas the A_{2A} and A_{2B} ARs are stimulatory to adenylyl cyclase via G_s protein. Adenosine A1 receptor (A_1AR) activation can also activate several types of K^+ channels and mitogen-activated protein kinases (MAPK) via β,γ-subunits released from $G_{i/o}$ proteins, and also inhibits N-type Ca^{2+} currents via PTX-sensitive pathways [1]. A_1ARs are expressed in large numbers in the brain, as well as in peripheral tissues including kidney, heart and liver [2]. Because of adenosine exerting different physiological effects, a large number of A_1AR antagonists exhibit a plethora of actions including anti-hypertensive, anti-depressive, anti-diabetic, anti-Parkinson and anti-hyperanalgesic effects [3]. In the kidney, the importance of A_1ARs has been confirmed in regulation of fluid balance [4]. Induction of diuresis and natriuresis without reducing renal function is therapeutically desirable in treatment of patients with renal dysfunction. Therefore, a large number of potent and selective A_1AR antagonists with structural diversity have been developed, including xanthinic or non-xanthinic scaffolds [5]. However, relatively few molecular entities have been realized in clinical application, mainly because of unsatisfactory pharmacokinetic properties and the complications of species differences between humans and animals, as well as differences in expression pattern of second

Min Lu and Bo Wang contributed equally to this work.

Electronic supplementary material The online version of this article (doi:10.1007/s11302-014-9424-5) contains supplementary material, which is available to authorized users.

M. Lu · B. Wang · C. Zhang · X. Zhuang · M. Yuan · H. Wang · W. Li · R. Su · J. Li (✉)
Beijing Institute of Pharmacology and Toxicology, 27th Taiping Road, Beijing 100850, China
e-mail: jinli9802@163.com

messenger systems [6]. Pharmacological differences in terms of neutral antagonists and inverse agonists, however, have been determined [7]. In the AR research field, 1,3-dipropyl-8-cyclopentylxanthine (DPCPX, an agent with a xanthinic scaffold) is widely used as a reference A_1R antagonist in preclinical studies. Interestingly, DPCPX has been identified as an inverse agonist in different systems with constitutive A_1R activity [8, 9]. Rolofylline (KW3902, a more selective and potent A_1R antagonist) also acts as an adenosine A_1R inverse agonist to inhibit osteoclast differentiation.

Inverse agonists and neutral antagonists were thought to act via different signal transduction mechanisms. Despite these obstacles, potent and selective non-xanthinic selective A_1AR antagonists with favourable pharmacokinetic properties draw the investigators' attention because of their many potential therapeutic applications. Most of the non-xanthinic adenosine receptor antagonists are nitrogen-containing heterocyclic compounds. In our laboratory, a series of novel tricyclic heteroaromatic derivatives were designed and synthesized. Based on the 3D-QSAR model derived from the quantitative structure–activity relationship analysis of a set of imidazo[1,2-a]quinoxaline molecules [10] with structural diversity, some important structural insights into the interaction between non-xanthinic ligands with A_1AR have been obtained, including hydrophobic interactions, hydrogen bond acceptors and hydrogen bond donors. Aided by this important structural information, a series of novel 4-alkylamino substitution 2-arylpyrazolo[4,3-c]quinolin-3-one derivatives were designed and synthesized in our laboratory. The biological activity study of these tricyclic heteroaromatic derivatives was focused on the evaluation of selectivity of A_1AR as an antagonist. A potent and selective A_1AR antagonist, 4-butylamino-2- (3-fluorophenyl)[4, 3-c]quinolin-3-one (PQ-69), was identified through receptor radioligand binding assay. In the present study, we studied PQ-69 affinity to A_1, A_{2A} and A_3 AR and selectivity between A_1AR and $A_{2A}AR$ in radioligand binding assay, and post-receptor G protein coupling properties of PQ-69 in cell lines stably expressing the human A_1AR. Further, we observed the inverse agonist activity of PQ-69 compared with DPCPX in cell lines. We also evaluated PQ-69 antagonist activity on isolated guinea pig tracheal strips. Furthermore, we found that PQ-69 displayed diuresis and natriuresis bioactivities in in vivo studies using normal rats.

Materials and methods

Chemistry

Solvents and reagents were commercially purchased from Sigma-Aldrich Chemical Company unless otherwise noted. All reactions were monitored by thin layer chromatography (TLC) on 25×75 mm glass slides precoated with silica gel (GF_{254}) to a thickness of 0.25 mm and viewed at 254-nm UV light. Column chromatography for product purification was performed using silica gel of 200–300 mesh. Melting points (mp) were determined using a RY-1 apparatus and are uncorrected. Hydrogen-1 NMR (^{1}H NMR) spectra were recorded on Varian Unity Inova 600 MHz and JNM-ECA-400 400 MHz instrument. The chemical shifts are reported in δ (ppm) and are relative to the central peak of the solvent that is always DMSO-d6. Mass spectra were obtained from Micromass ZabSpec and API3000 instruments. Elemental analysis for N, H and N was performed with CarloErba-1106 and the results were within ±0.5 % of the theoretical unless otherwise stated. All reported compounds show ^{1}H NMR and mass spectra in agreement with the assigned structures.

General method for the synthesis of PQ-69 and its analogues

2,4-Dihydroxy-3-quinolinecarboxylic acid ethyl ester and its analogues (II) To gain a solution of diethyl malonate (0.78 mol) in dry matter of fermented filtrate (DMF) (120 mL), sodium hydride (0.31 mol) was added partwise at room temperature. The suspension was stirred 30 min at 70 °C and the solution of isatoic anhydride (0.26 mol) in DMF (250 mL) was added dropwise during 1 h. The mixture was stirred for 5 h at 120 °C. After the resulting mixture was cooled to 0 °C, the precipitant was collected through filtering and dissolved with 200-mL H_2O. The DMF filtrate was concentrated under reduced pressure and the resulting residue was also dissolved with 150-mL H_2O. The combined aqueous phase was adjusted by HCl until the pH value was between 3–4, the resulting precipitant was collected and washed with water and dried under ambient condition. The crude was recrystallized by using ethyl acetate to afford II (44 g, 73 % yield) as pale yellow crystal, m.p. 206–208 °C.

2,4-Dichloro-3-quinolinecarboxylic acid ethyl ester and its analogues (III) A mixture of compounds (II) (0.12 mol), phosphorus oxychloride (160 mL) and phosphorus pentachloride (5 g) was stirred at 100–115 °C for 3 h. Evaporation of the excess phosphorus oxychloride at reduced pressure gave a residue that was treated with ice water (500 mL). The aqueous solution was extracted twice with dichloromethane (250 mL). The combined organic phase was dried over $MgSO_4$, filtered and concentrated under reduced pressure. The solid was recrystallized by using ethyl acetate to afford III (26.2 g, 80.5 % yield) as pale yellow crystal, m.p. 100–101 °C.

2-Alkylamino substituted 4-chloride-3-quinolinecarboxylic acid ethyl ester and its analogues (IV) A mixture of 2,4-dichloro compounds (III) (40 mmol) and n-butylamine (160 mmol) in methanol (120 mL) was refluxed for 8 h. The reaction mixture was concentrated under reduced pressure and the resulting residue was purified using silica gel column chromatography (CH_2Cl_2/MeOH=10:1) to afford IV (7.8 g, 63.2 % yield) as a pale yellow waxy solid.

PQ-69 and its analogues (V) To gain a solution of compounds (IV) (1.5 mmol) in ethanol (30 mL), a mixture of 3-fluorophenylhydrazine (4.5 mmol) and triethylamine (4.5 mmol) in ethanol (20 mL) was added dropwise. The reaction mixture was refluxed under N_2 for 24 h and concentrated under reduced pressure and the resulting residue was subjected to purification using silica gel column chromatography (CH_2Cl_2/MeOH=50:1) to afford PQ-69 (0.16 g, 30.8 % yield) as a white crystal, m.p. 204–206 °C.

Chemicals

Dulbecco's modified Eagle medium with nutrient mixture F12 (DMEM/F12) medium, foetal calf serum and geneticin (G418) were obtained from Gibco (Grand Island, NY, USA). Guanosine-5′-O-(3-[^{35}S]-thio) triphosphate ([^{35}S]-GTPγS), [^{3}H]-1,3-dipropyl-8-cyclopentylxanthine([^{3}H]DPCPX), [^{3}H]-2-[[4-(2-carboxyethyl)phenethyl]-amino]-5-(N-ethyl-carbamoyl)adenosine ([^{3}H]CGS21680) and N^6-(3-[^{125}I]iodo-4-aminobenzyl-5′-Nmethylcarboxamido

Adenosine ([^{125}I]-AB-MECA) were obtained from PerkinElmer Life & Analytical Sciences (Boston, MA, USA). Adenosine deaminase (ADA), guanosine diphosphate (GDP), GTPγS, (R)-N^6-(1-methyl-2-phenylethyl) adenosine (R-PIA), 5′-(N-ethylcarboxamido) adenosine (NECA), 2-chloro-N^6-cyclopentyl adenosine (CCPA), 1,3-dipropyl-8-cyclopentylxanthine (DPCPX), forskolin, histamine, furosemide (FURO), hydrochlorothiazide (HCTZ), polyethyleneglycol 400 (PEG400), internal standard solution, NADPH and all other reagents were purchased from Sigma-Aldrich (St. Louis, MO, USA). Acetonitrile and other reagents used in pharmacokinetic evaluation were all of analytical grade (J&K Chemical Ltd., Beijing, China). Pooled human liver microsomes (protein content of 20 g/L, batch no. 18888) were purchased from BD Gentest (Woburn, MA, USA). Rat liver microsomes were prepared by differential centrifugation [11], and the protein concentration of the microsomes was determined using the Lowry method.

Cell culture

Chinese hamster ovary cells (CHO) and human embryonic kidney 293 cells (HEK-293) were, respectively, transfected with the recombinant hA$_1$AR, hA$_{2A}$AR and hA$_3$AR using the calcium phosphate precipitation. The CHO-hA$_1$, HEK-293-hA$_{2A}$ and CHO-hA$_3$ cells with the highest expression level were cultured in DMEM/F12 medium containing 10 % foetal calf serum, 100 IU/mL penicillin, 100 μg/mL streptomycin, 2 mM L-glutamine and 400 μg/mL geneticin at 37 °C in 5 % CO_2/95 % air.

Membrane preparation

Cell membranes were prepared as previously described with slight modification [12]. After washing twice with ice-cold phosphate-buffered saline, the cultured cells were detached by incubation with Versene buffer (137 mM NaCl, 2.7 mM KCl, 1.5 mM KH_2PO_4, 10 mM $Na_2HPO_4{\cdot}12\ H_2O$, 1 mM glucose·H_2O, 2 mM EDTA-$Na_2{\cdot}2\ H_2O$, pH 7.4) and collected by centrifugation at 1,000×g for 10 min.

The cell pellet was suspended in ice-cold homogenization buffer (5 mM Tris/HCl, 5 mM EDTA-$Na_2{\cdot}2\ H_2O$, 5 mM EGTA, 0.1 mM PMSF, pH 7.4) for 20 min and then centrifuged at 40,000×g for 10 min at 4 °C. The membrane pellet was resuspended in 50 mM Tris/HCl buffer (pH 7.4) and centrifuged at 40,000×g for 10 min at 4 °C. The final pellets were resuspended in reaction buffer (50 mM Tris/HCl, 2 mM $MgCl_2$, pH 7.4). The protein concentration of the membranes was measured by the Bradford method and aliquots were stored at −80 °C.

Radioligand binding assay

Radioligand binding assay was performed using a slightly modified protocol by Klotz et al. [12]. Thawed membranes containing 30 μg CHO-hA$_1$ or 50 μg HEK-293-hA$_{2A}$ and 100 μg CHO-hA$_3$ membranes were incubated in reaction buffer containing 2 U/ml adenosine deaminase. A range of concentrations of [^{3}H]-DPCPX (0.0625–4 nM), [^{3}H]-CGS21680 (0.9375–60 nM) or [^{125}I]AB-MECA (0.25–4 nM) were used to construct saturation-binding curves to determine receptor binding activity on transfected cells and an optimal concentration of [^{3}H]-DPCPX, [^{3}H]-CGS21680 or [^{125}I]AB-MECA was used in subsequent PQ-69 or DPCPX receptor binding assays. The effect of PQ-69 or DPCPX on [^{3}H]-DPCPX, [^{3}H]-CGS21680 binding to cell membranes was determined in the presence of 1 nM [^{3}H]-DPCPX, 15 nM [^{3}H]-CGS21680 or 0.5 nM [^{125}I]AB-MECA and varying concentrations of PQ-69 or DPCPX (10^{-11}–10^{-5} M). After 1-h incubation at 37 °C, the reaction was terminated by filtration through Whatman GF/C filters pre-soaked in 50 mM Tris/HCl for 30 min. Nonspecific binding was determined in the presence of 1 nM [^{3}H]-DPCPX and 10 μM R-PIA, 15 nM [^{3}H]-CGS21680 and 10 μM NECA or 0.5 nM [^{125}I]AB-MECA and 10 μM R-PIA. Specific receptor binding was calculated by subtracting nonspecific binding from total

ligand binding. The receptor binding data were analyzed using a non-linear regression model (GraphPad Software, San Diego, CA, USA). IC_{50} values of PQ-69 or DPCPX were determined using the method described by Cheng and Prusoff [13]. K_i values were calculated using the equation $K_i = IC_{50}/(1+[S]/K_d)$ ([S] is the concentration of radioligand and K_d is dissociation constant; Cheng & Prusoff [13]). All data are presented as mean values of two or three separate experiments.

[^{35}S]-GTPγS binding assay

A_1AR-mediated modulation of G protein activity was determined using [^{35}S]-GTPγS binding. Briefly, membranes (50 μg) were incubated in reaction buffer (20 mM HEPES, 3 mM $MgCl_2$, 100 mM NaCl, pH 7.4) containing 0.2 nM [^{35}S]-GTPγS, 10 μM GDP and 2 U/ml ADA at 37 °C for 1 h. Binding of [^{35}S]-GTPγS in the presence of 40 μM GTPγS was considered to be nonspecific binding. The intrinsic activity of PQ-69 or DPCPX alone on [^{35}S]-GTPγS binding was measured in the absence of R-PIA. The effect of compounds on 0.1 μM R-PIA stimulated [^{35}S]-GTPγS binding was measured in the presence of varying concentrations of PQ-69 or DPCPX (10^{-11}–10^{-5} M). Assays were terminated with rapid filtration onto Whatman GF/B filters, which were pre-soaked with 50 mM Tris/HCl containing 5 mM $MgCl_2$. Filters were dried, and the radioactivity retained on the filters was determined by a scintillation spectrometer (LS6500; Beckman, CA, USA). GraphPad Prism software was used to calculate EC_{50} values of R-PIA stimulated [^{35}S]GTPγS binding and IC_{50} values of PQ-69 or DPCPX on R-PIA stimulated [^{35}S]GTPγS binding.

Cyclic AMP accumulation assay

Cyclic adenosine monophosphate (cAMP) measurements were performed according to the handbook of the cAMP dynamic 2 kit (Cisbio, Bedfold, MA, USA). Briefly, cells were detached by incubation with Versene buffer and dispensed into 384 wells in modified Hank's Balanced Salt Solution (Sigma-Aldrich, Co.) buffer containing 0.1 % glucose and 0.5 mM IBMX. For A_1AR coupled to G_i protein, the total reaction volume (20 μL) containing 5,000 cells/well and 4 μM forskolin was used to raise cAMP levels. A series of concentrations of PQ-69 or DPCPX (10^{-11}–10^{-5} M) were added to the cells to measure the effect of compounds on basal cAMP levels. For the measurement of antagonist activity, a selective A_1AR agonist, 50 nM CCPA, was added to inhibit forskolin-induced cAMP accumulation before the addition of PQ-69 or DPCPX (10^{-11}–10^{-5} M). Each compound described above, when added to cells, required 30-min incubation at room temperature in the dark. Finally, cAMP levels were measured using homogeneous time-resolved fluorescence technology in an EnVision® 2104 Multilabel Reader (PerkinElmer Inc., Waltham, MA, USA) and the ratio of the signal at 665 and 615 nm was determined. Results were measured and expressed in delta *F*% according to the manufacturer. The concentration of cAMP was acquired by a standard curve plotting delta *F*% values against the log values of cAMP concentration. IC_{50} was calculated by non-linear regression using GraphPad Prism software.

Measurement of pA2 values

Male Dunkin-Hartley guinea pigs (350–400 g) were stunned and the trachea rapidly removed and placed in modified Kreb's solution (118 mM NaCl, 4.7 mM KCl, 3.4 mM $CaCl_2$, 1.2 mM KH_2PO_4, 1.2 mM $MgSO_4$, 25 mM Na_2CO_3, 10 mM glucose). Following removal of fat and connective tissue, spiral strips consisting of two adjacent cartilage rings were prepared and suspended in a tissue chamber containing Kreb's solution at 37 °C, bubbled with 95 % O_2 and 5 % CO_2. Tracheal preparations were connected to force displacement transducers for measuring isometric tension responses. Tracheal preparations were equilibrated for 60 min maintaining a resting tension of 1 g and washed with Kreb's solution every 15 min before specific experimental protocols were initiated.

To ascertain tissue viability, a contraction of acetylcholine (ACh, 10^{-6} M) to 80 % of maximal tension was constructed before each experiment. Following washout and recovery of basal tone, increasing concentrations of CCPA (10^{-9}–10^{-5} M) were added cumulatively to construct the first agonist concentration–response curve. After an initial equilibration period of about 60 min, the subsequent cumulative concentration–response curves to CCPA were constructed after 30-min preincubation with DPCPX (10^{-5}, 3×10^{-5}, 6×10^{-5} M) or PQ-69 (1×10^{-6}, 3×10^{-6}, 9×10^{-6} M). One antagonist concentration was examined in each preparation, and the effects of different concentrations of PQ-69 or DPCPX were tested in different tissues from the same animal. The pA2 values for DPCPX and PQ-69 were calculated as described by Arunlakshana and Schild [14]. The 50 % effective concentration (EC_{50}) of CCPA was estimated by non-linear regression in the absence or presence of DPCPX and PQ-69. Schild plot analysis was performed in each preparation using these EC_{50} values and the pA2 values were calculated from linear regression.

Preliminary pharmacokinetic evaluation

PQ-69 and DPCPX (2 mg/kg) were intravenously administered in rats. The dosing solutions of PQ-69 and DPCPX were prepared in 65 % PEG400 and 35 % saline. Serial

blood samples were collected at various times and centrifuged to obtain plasma. For sample analysis, 50 μL of plasma was added to 10 of acetonitrile and 150 μL of internal standard solution. The mixture was centrifuged at 18,800×*g*, 4 °C for 10 min. The supernatant was then analyzed using high-performance liquid chromatography tandem mass spectrometry (LC-MS/MS). The pharmacokinetic parameters were calculated using a noncompartmental model in WinNonlin Professional (Version 5.2.1, Pharsight Corp; Mountain View, CA, USA). In vitro metabolic stability of PQ-69 and DPCPX was investigated using rat and human liver microsomes in procedures similar to those previously described [15]. The incubations (5 μM parent drug, 0.5 mg/ml microsomal protein, 0.1 M phosphate buffer) were started by the addition of 1 mM NADPH solution after a 5-min preincubation at 37 °C and were terminated after 60 min. The amount of parent drug was analyzed by LC-MS/MS and the percent of remaining parent drug was calculated and compared. In vitro permeabilities of PQ-69 and DPCPX were carried out using a Caco-2 cell line, according to previously described methods [16]. In brief, drug solution (5 μM) was placed in the donor chamber and samples were taken from the receptor chamber at 90 min. Samples were analyzed by LC-MS/MS, then the apparent permeability coefficient (P_{app}) was calculated using the equation: $P_{app}=(dQ/dt)/(A\times C0)$.

Diuretic effects in normal rats

Male Sprague–Dawley (SD) rats, weighing 200–300 g, were used in the present study. The animals were kept at 25 °C in a 12-h light–dark cycle. They had free access to food and water. Animal care and procedures were strictly in accordance with *The Guide for the Care and Use of Laboratory Animals of the National Institutes of Health*. Diuretic effects of compounds in normal rats were determined with a slight modification of the previous method [17]. In brief, rats were fasted for 24 h, and the drug suspension or the vehicle (EtOH/PEG400/H_2O=1:5:4) was intravenously administered to the rat at a volume of 4 ml/kg. After the administration, rats were housed individually in metabolic cages without food and water. Urine was collected every 4 h, and the urinary volume and concentration of sodium in the urine were measured.

Data and statistical analysis

Data were expressed as mean±S.E.M. Statistical analysis of experiments was performed using Prism software (Graph Pad software) including unpaired Student's *t* test for two-group comparison and one-way ANOVA with Tukey's multiple comparison test for multiple group comparisons. *P* values less than 0.05 were regarded as statistically significant.

Results

Chemistry

Aided by the 3D structural insights into the interaction between non-xanthinic ligands with A_1AR [12], a series of novel 4-alkylamino substitution 2-arylpyrazolo[4,3-c]quinolin-3-one derivatives were designed and synthesized. PQ-69 and its analogues (Supplementary Table 1) were prepared according to the procedure depicted in Scheme 1. Various commercially available isatoic anhydride (I) as starting material were reacted with sodium hydride followed by diethyl malonate in DMF at 120 °C to afford 2,4-dihydroxy-3-quinolinecarboxylic acid ethyl ester derivatives (II) in moderate yield. Compounds (II) upon treatment with phosphorus oxychloride and phosphorus pentachloride at 110 °C gave the unstable 2,4-dichloro-3-quinolinecarboxylic acid ethyl ester derivatives (III) in good yield. Reaction of 2,4-dichloro compounds (III) with appropriate amines in refluxing methanol afforded 2-alkylamino substituted 4-chloride-3-quinolinecarboxylic acid ethyl ester (IV) 4-chloro of which was replaced with appropriately substituted phenylhydrazine and simultaneously cyclized to target compounds(V) in refluxing ethanol, which were purified by column chromatography on silica gel.

Pharmacology

Identification and characterization of the PQ-69 molecule

The preliminary results of the receptor radioligand binding assay revealed a hit from this class of compounds with good affinity for the A_1AR. Investigated compounds for affinity at hA_1, hA_{2A} and hA_3 ARs expressed on CHO or HEK293 cells were listed in Table 1, demonstrating that PQ-69 had the highest binding affinity for the A_1AR over other adenosine receptors. In comparison with DPCPX, the K_i value of PQ-69 on A_1AR was 0.96 nM, which was lower than that of DPCPX (1.9 nM in our current study). By contrast, the K_i values of PQ-69 and DPCPX for A_{2A}AR were 208 and 100 nM, respectively. The selectivity of PQ-69 on A_1AR over A_{2A}AR was 217-fold, which is much higher than that of DPCPX (52-fold). These results suggested that PQ-69 has higher affinity and selectivity to A_1AR than DPCPX. Interestingly, we found a 13-fold increase in affinity of PQ-69 for rat brain membrane A_1AR to the human A_1AR, with K_i values of 0.07 nM (data not shown).

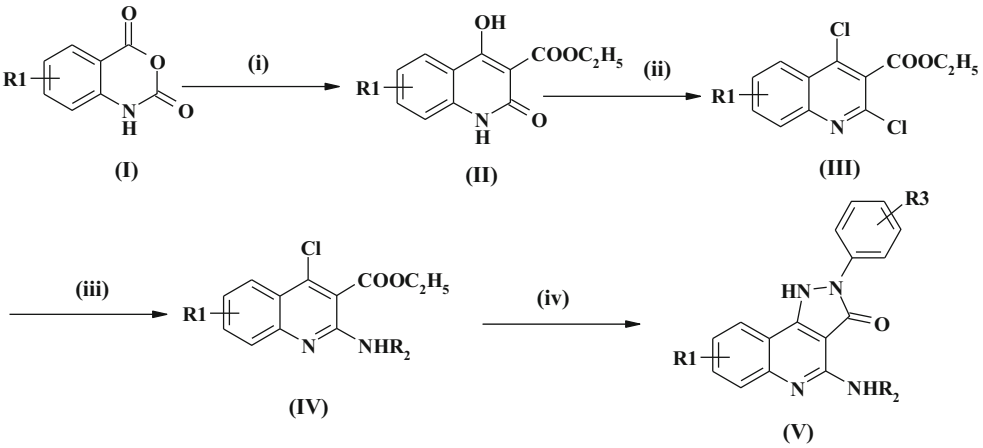

Scheme 1 Synthesis of PQ-69 and its analogues. Reagents and conditions: *i* NaH/DMF, Dimethyl manolate, 120 °C; *ii* Phosphorus oxychloride/ phosphorus pentachloride, 100 °C; *iii* R_2NH_2/MeOH, reflux; *iv* Substituted phenylhydrazines/ EtOH, reflux

Pharmacological studies of PQ-69 compared with DPCPX in vitro

Antagonist and inverse agonist effects on G protein activation of PQ-69 compared with DPCPX We next measured the ability of PQ-69 and DPCPX on G protein activation in CHO-*h*A_1AR cells in a [^{35}S]-GTPγS binding experiment. In the absence of R-PIA, a selective A_1AR agonist, we found that PQ-69 significantly inhibited basal [^{35}S]-GTPγS binding, similar to the effect seen with DPCPX (Fig. 1a). R-PIA further increased the basal binding of [^{35}S]-GTPγS (100 %) to 347 %. By contrast, PQ-69 and DPCPX reduced the basal binding of [^{35}S]-GTPγS in a concentration-dependent manner with IC_{50} values of 0.19 and 7.84 nM, respectively. At a concentration of 1 μM, PQ-69 and DPCPX significantly reduced the basal binding of [^{35}S]-GTPγS by 44.6 and 56.9 %, respectively, suggesting that PQ-69 might be an inverse agonist for A_1AR. We then measured the ability of PQ-69 and DPCPX to reverse the activation effect of R-PIA on G proteins in CHO-hA_1AR cells. Figure 1b illustrated the inhibitory effects of PQ-69 and DPCPX on the increase in the binding of [^{35}S]-GTPγS induced by R-PIA (0.1 μM). PQ-69

Table 1 Structure and affinity binding properties of DPCPX, PQ-69 and its analogues at human recombinant A_1, A_{2A} and A_3 adenosine receptors

Cpd	Substituents			K$_i$, nM			A_1AR selectivity
	R1	R2	R3	A_1[a]	A_{2A}[b]	A_3[c]	(A_{2A}/A_1)
DCPCX				1.90±0.3	100±0.2	>10^5	52.6
PQ-69	7-H 8-H	n-C4H9	3′-F	0.95±0.2	208±0.3	>10^5	217
PQ-83	7-OCH3 8-OCH3	n-C4H9	3′-F	0.90±0.3	109±0.2	>10^5	120
PQ-85	7-OCH3 8-OCH3	n-C4H9	4′-F	1.57±0.2	52.6±0.3	>1000	33.6
PQ-86	7-OCH3 8-OCH3	n-C4H9	4′-Br	7.07±0.2	247±0.2	>1,000	35
PQ-88	7-H 8-Cl	n-C4H9	3′-Br	55.8±0.2	>1,000	>1,000	22.2
PQ-103	7-H 8-H	n-C3H7	3′-F	1.54±0.3	154±0.3	>10^5	100
PQ-107	7-H 8-H	n-C4H9	H	1.07±0.2	170±0.4	>10^5	159

[a] Displacement of specific [^{3}H]DPCPX binding in CHO cells transfected with human recombinant A_1AR

[b] Displacement of specific [^{3}H]CGS21680 binding in HEK-293 cells transfected with human recombinant A_{2A}AR

[c] Displacement of specific [^{125}I]AB-MECA binding in CHO cells transfected with human recombinant A_3AR

Values are mean±standard error of three separate experiments

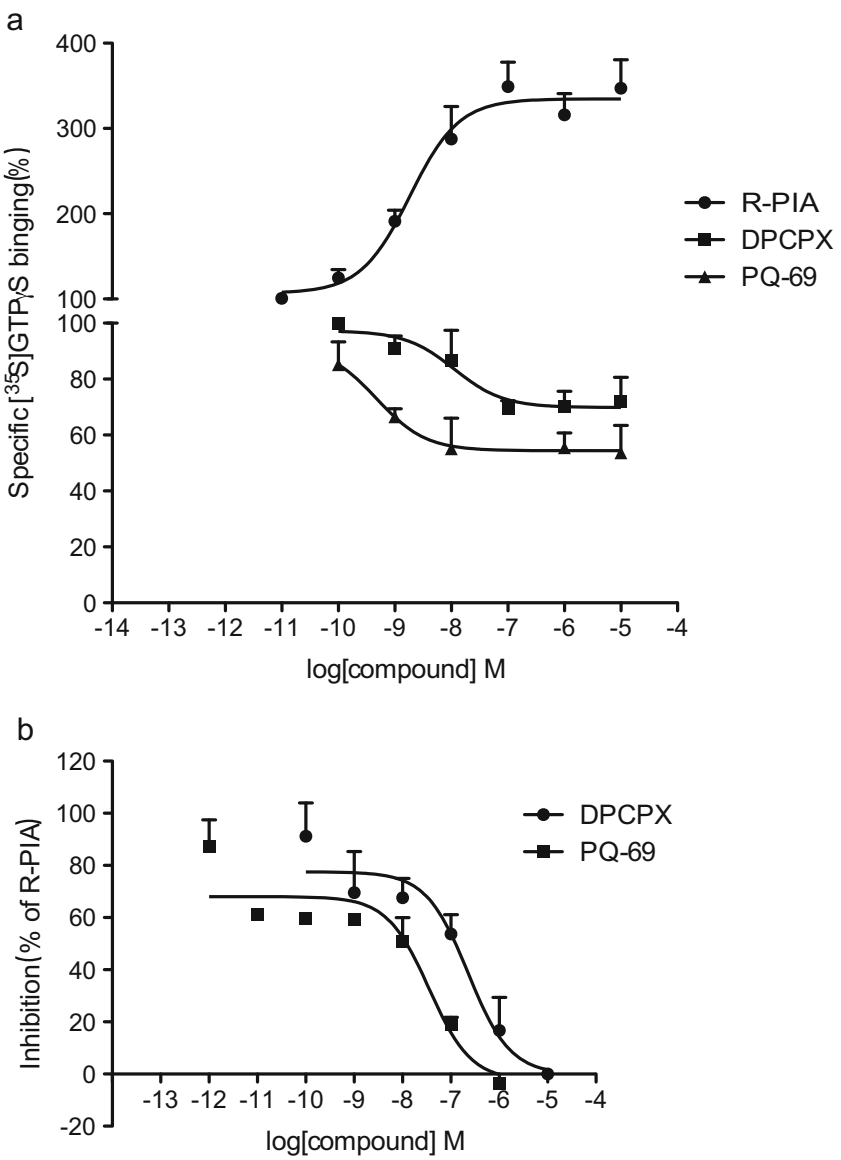

Fig. 1 Effects of A_1AR ligands on specific binding of [^{35}S]-GTPγS to membranes prepared from CHO cells expressing the recombinant human A_1AR. **a** R-PIA induced an increase in basal [^{35}S]-GTPγS binding; DPCPX and PQ-69 induced a decrease in basal [^{35}S]-GTPγS binding. **b** Attenuation of the 0.1 μM R-PIA induced increase in [^{35}S]-GTPγS binding by DPCPX and PQ-69. All data are mean±S.E.M from three independent experiments, performed in duplicate. *Curves* were fitted using dose–response analysis

decreased the specific binding of [^{35}S]-GTPγS in a concentration-dependent manner, with an IC_{50} value of 18.3 nM, which was 12-fold lower than that of DPCPX (227.2 nM), suggesting that PQ-69 was more potent than DPCPX in antagonizing the R-PIA-induced G protein activation.

Antagonistic effect and inverse agonistic activity of PQ-69 compared with DPCPX on cAMP response To further demonstrate the characteristic of antagonists with inverse agonist activity, the effects of the compounds on cAMP contents of intact CHO-*h*A_1AR cells were observed. As shown in Fig. 2a, CCPA, a selective A_1AR agonist inhibited the forskolin-stimulated cAMP accumulation in a concentration-dependent manner with an EC_{50} of 16.5 nM. By contrast, PQ-69 or DPCPX increased intracellular cAMP concentration in a concentration-dependent manner after 1 μM forskolin stimulation with an IC_{50} of 38.4 and 315 nM, respectively. PQ-69 or DPCPX reversed the inhibitory effects of CCPA (50 nM) on cAMP concentration with IC_{50} values of 143.8 and 272.3 nM, respectively (Fig. 2b). It was also found that PQ-69 and DPCPX had very weak effects on the inhibitory action of NECA (10 μM) on cAMP concentration in HEK-293-*h*A_{2A}AR cells with IC_{50} values of 3.5 and 1.56 μM, respectively (data not shown). These results suggested that PQ-69 and DPCPX were both selective A_1AR antagonists with inverse activities, but PQ-69 was more potent than DPCPX.

Antagonist action of PQ-69 compared with DPCPX on contractive responses of isolated guinea pig trachea induced by CCPA

In isolated guinea pig trachea, CCPA-induced contractile responses in a concentration-dependent manner (0.01–10 μM). pA2 values and Schild plots have been shown in Table 2.

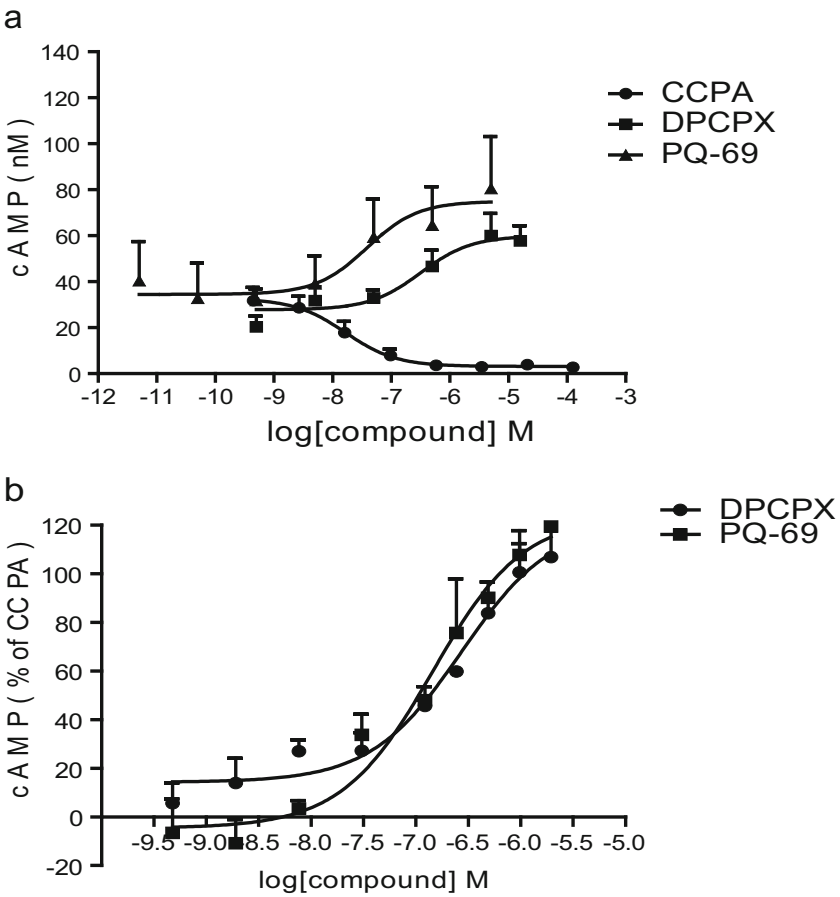

Fig. 2 Effects of A_1AR ligands on cAMP production in CHO cells expressing the recombinant human A_1AR. **a** Comparison of cAMP concentration by DPCPX, PQ-69 and CCPA in 1 μM forskolin-stimulated cells. **b** Antagonism of 100 nM CCPA-induced activation of forskolin-stimulated cells by DPCPX and PQ-69. cAMP production is given as percentage of CCPA-induced decrease. All data are the mean±S.E.M from at least three independent experiments, performed in duplicate. *Curves* were fitted with dose–response analysis

Schild plots of DPCPX and PQ-69 were not significantly different from unity. Affinity estimates (pA2 values) of PQ-69 were slightly different from that of DPCPX. PQ-69 was slightly more potent with a pA2 value of 8.99 than that of DPCPX (8.11). This finding indicated that PQ-69 was a potent competitive antagonist on CCPA-induced tracheal contraction.

Pharmacokinetic studies

The pharmacokinetic profiles of PQ-69 and DPCPX were first determined in SD rats after intravenous administration. As shown in Table 3, PQ-69 displayed longer terminal elimination half-life ($t_{1/2}$) with 7.92 h compared with 2.36 h for DPCPX. However, the total plasma clearance of PQ-69 was similar to DPCPX. Furthermore, a larger volume of distribution was found for PQ-69 with 25.5 L/kg compared with DPCPX (7.11 L/kg). By contrast, PQ-69 displayed better metabolic stability and broader tissue distribution than DPCPX. Therefore, the large tissue distribution balanced the slow metabolism. For subsequent experiments, the difference in liver metabolism was also evaluated using an in vitro microsomal stability assay. After 60 min incubation in rat liver microsomes, the percentage of remaining parent drugs was significantly different between PQ-69 (73.5±2.6 %) and DPCPX (30.1±3.4 %). Therefore, we have shown that PQ-69 displayed better metabolic stability in rat liver microsomes compared with DPCPX. The absorptive permeability (P_{app}) of PQ-69 was measured using a Caco-2 transport assay. The results indicated that both PQ-69 and DPCPX had moderate permeability across epithelial cells.

Table 2 Effects of antagonists on CCPA-induced contractions of guinea pig isolated tracheal strips. pA2 values are given as mean±S.E.M and determined in at least four independent experiments

Compound	pA2	SchildSlope	Number (*n*)
DPCPX	8.11±0.13	1.19	5
PQ-69	8.99±0.2	1.28	4

Diuretic effects in normal rats

Finally, we observed the diuretic effect and natriuretic effect of PQ-69 in normal rats compared with DPCPX, FURO and HCTZ. In Fig. 3a, PQ-69 (0.03, 0.3, 3 mg/kg) significantly increased urine flow by 82–162 % compared with that in the vehicle group. DPCPX (1 mg/kg), HCTZ (1 mg/kg) and

Table 3 Pharmacokinetic and metabolic stability results for DPCPX and PQ-69 in SD rats. Intravenous administration of DPCPX and PQ-69 (2 mg/kg) occurred in 65 % PEG400 and 35 % saline

Compound	PK parameters		Remaining parent drug		Caco-2 cell permeability
	$t_{1/2}$ (h)	Vss (L/Kg)	RLM (%)	HLM (%)	P_{app} ($\times 10^{-6}$)
PQ-69	7.92±6.60	25.5±21.5	73.5±2.6	87.4±2.7	19.4±2.5
DPCPX	2.36±1.47	7.11±5.42	30.1±3.4	62.6±2.0	20.4±0.9

FURO (6 mg/kg) also significantly increased urine flow by 133, 114 and 289 % compared with that in the vehicle group, respectively. A significant diuresis occurred at lower doses of PQ-69 (0.03 mg/kg). FURO (6 mg/kg) with a urine volume of 35.2 ml/kg/4 h was twice as potent a diuretic as PQ-69 (0.03 mg/kg) with a urine volume of 16.4 mL/kg/4 h, and HCTZ (1 mg/kg) with a urine volume of 19.4 mL/kg/4 h. The effect of PQ-69 (0.3 mg/kg) was equal to DPCPX (1 mg/kg) and slightly higher than HCTZ (1 mg/kg), with a urine volume of 20.2, 21.0 and 19.4 mL/kg/4 h, respectively.

As shown in Fig. 3b, the concentration of sodium increased significantly in all the drug-treated groups compared with the vehicle group. Sodium concentration was increased by 120–306 % in rats treated with PQ-69 (0.03, 0.3, 3 mg/kg), by 162 % in rats treated with DPCPX (1 mg/kg), by 214 % in rats treated with HCTZ (1 mg/kg) and by 214 % in rats treated with FURO (6 mg/kg). FURO (6 mg/kg) caused significantly greater renal excretion of sodium than PQ-69, DPCPX or HCTZ at higher doses. The natriuretic activity of PQ-69 (0.3 mg/kg) was similar to HCTZ (1 mg/kg) with urinary Na^+ of 1.6 and 1.78 mmol/kg/4 h, respectively; meanwhile, PQ-69 (3 mg/kg) was equivalent to DPCPX (1 mg/kg) with urinary Na^+ of 2.33 and 2.19 mmol/kg/4 h, respectively.

Discussion

To identify potent and A_1AR-selective antagonists, we have designed and synthesized a series of novel 4-substituent-2-arylpyrazolo[4,3-c]quinolin-3-one derivatives. On the basis of knowledge obtained from the lead optimization project, a putative structure–activity relationship model was proposed. (i) A common feature of these compounds with A_1AR affinities is a quinofused five-member nitrogen-containing heterocyclic nucleus as a template, with aromatic or π electron-rich planar molecular architecture. (ii) The substituents, i.e. 2-aryl, 3-carbonyl and 4-alkylamino, are indispensable structural factors for making the compounds biologically active. (iii) The specific substituents in the specific positions of the three aromatic rings have a synergistic effect on the contributions to the biological activity of the compounds. That is, the affinities to A_1AR of compounds are the result of the three sets of substituents acting together. (iv) At the same time, the substituents appended on the quinoline ring, 2-aryl as well as 4-alkylamino, largely contribute to the solubility of compounds.

PQ-69 was identified as a result of radioligand binding assay, ex vivo and in vivo biological evaluations together with a thorough lead optimization programme. PQ-69 was identified as an ideal candidate for further research showing nearly a fourfold longer $t_{1/2}$ than that of DPCPX in rats and also better metabolic stability in the human hepatic microsomal enzyme incubation experiment in vitro (Table 3), suggesting that PQ-69 has even better pharmacokinetic properties than DPCPX.

In the present study, the pharmacological profiles of PQ-69 were evaluated through various in vivo and in vitro

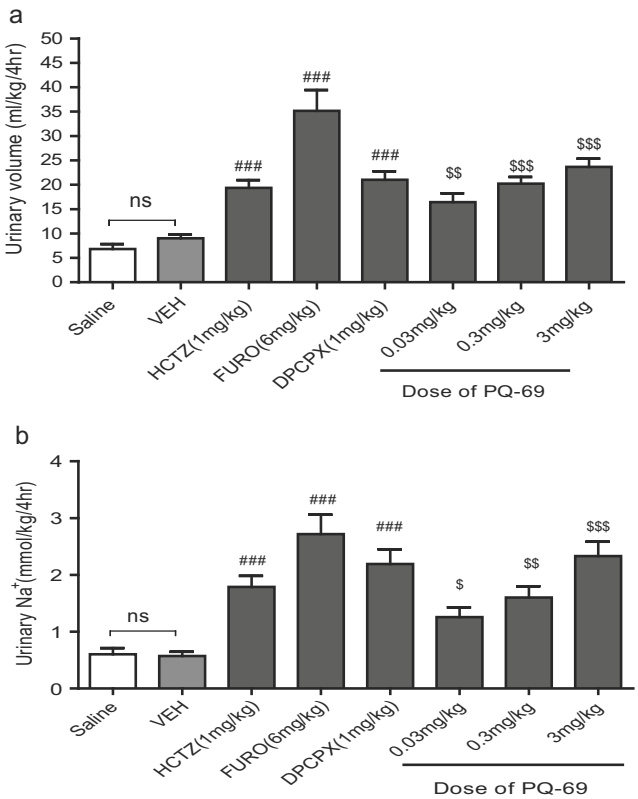

Fig. 3 The diuretic and natriuretic effects of PQ-69 and DPCPX in normal rats. **a** Diuretic responses to PQ-69, DPCPX, FURO and HCTZ in normal rats. Results are expressed as the mean±S.E.M. and represent the average values of urine collections during the 4 h following each dose. **b** Natriuretic activity of PQ-69, DPCPX, FURO and HCTZ in normal rats. Results are expressed as the mean±S.E.M. and represent the average values of urine Na^+ content during the 4 h following each dose. $^{###}p<0.001$ vs Veh, unpaired *t* test; $^{\$\$}p<0.01$, $^{\$\$\$}p<0.001$ vs Veh, One-way ANOVA and Newman-Keuls multiple comparison test; $n=8$

experiments. Simultaneously, we performed all in vitro pharmacological studies on human A_1AR in view of apparent species differences between humans and rats. Consistent with previous studies, DPCPX displayed moderate affinity and selectivity for human A_1AR in a recombinant expressed human adenosine receptor mammalian cell system. The results from radioligand binding experiments revealed that PQ-69 displayed a more than twofold increase in A_1AR affinity and fourfold increase in A_1AR selectivity compared with those of DPCPX. Furthermore, even at a concentration of 0.1 μM, PQ-69 had no effect on the binding for α_{1A}- and α_{1B}-adrenoceptors, ß-adrenoceptors, dopamine D_1, D_2 and D_3 receptors or muscarinic M_4 and M_5 receptors overexpressed in CHO or HEK-293 cell line systems (data not shown).

In addition to activation of A_1AR-coupled $G_{i/o}$ protein, cAMP is the key molecule in reflecting A_1AR activation or antagonism. In this study, PQ-69 appeared to be a more potent antagonist than DPCPX in mammalian cells in functional [^{35}S]-GTPγS binding and cAMP assays. Moreover, we also found that PQ-69 exhibited higher selective antagonism at A_1AR than DPCPX with an IC_{50} at A_{2A} AR of 3.5 and 0.14 μM, respectively (data not shown).

Given that PQ-69 appeared to be a more potent and selective A_1AR antagonist than DPCPX in vitro, we tried to relate antagonist studies made in recombinant systems to more physiologically relevant settings, such as isolated tissues or in vivo studies. We further assessed the antagonizing activity of PQ-69 and DPCPX on CCPA-induced isolated guinea pig tracheal strips.

Both PQ-69 and DPCPX significantly antagonized the inhibition by CCPA of the contraction of tracheal strips. The higher pA2 value of PQ-69 in isolated guinea pig tracheal strips indicated higher antagonism compared with DPCPX. Moreover, PQ-69 was found to relax tonic contractions of guinea pig tracheal strips in a concentration-dependent manner (10^{-10}–10^{-6} M; data not shown) suggesting that the antagonism by PQ-69 was mediated by blockade of endogenous A_1AR. Therefore, the above results indicated that PQ-69 might be a potent and highly selective A_1AR antagonist. Interestingly, in this study, DPCPX was identified as an inverse agonist in a recombinant mammalian cell system, consistent with previous studies [9, 10]. DPCPX behaved as an inverse agonist by directly decreasing basal G protein activation and increasing intracellular cAMP in vitro tests. Moreover, compared with DPCPX, 16-fold more potent A_1AR inverse agonist activity of PQ-69 was detected in a [^{35}S]-GTPγS binding assay, but only 8-fold inverse agonist activity was seen when measuring increasing cAMP production. A possible explanation for our observation is that significant variation in cell culture is attributed to differences in expression patterns of second messenger systems. Therefore, PQ-69 is a selective antagonist and inverse agonist at the A_1AR. Notably, native systems are of particular importance for analysing the in vivo relevance of constitutive activity because these systems have physiological expression levels of target receptors. The exact inverse agonist property of PQ-69 needs further in vivo studies.

In this study, the bioactivity of PQ-69 became more potent as the experimental system advanced from the in vitro molecular level to the cellular level and then to in vivo experiments. DPCPX potently promoted diuresis and natriuresis at the dose of 0.1 mg/kg in anaesthetized rats, which results from the blockade of endogenous adenosine modification on renal excretory function via stimulation of the A_1AR subtype. In our study, PQ-69 increased urine flow and natriuresis at the dose of 0.03 mg/kg. PQ-69 and DPCPX both displayed similar diuretic efficacy to thiazide diuretics.

Levels of extracellular adenosine are usually enough to tonically activate inhibitory A_1ARs. Therefore, adenosine antagonists with improved therapeutic potential application mainly are dependent on the level of endogenous purinergic tone instead of the absolute distribution of receptors. Whether the more potent inverse agonist characteristics of PQ-69 were related to the diuretic effects in the kidney remains to be determined. Thus, to elucidate whether PQ-69 is either a true antagonist or inverse agonist requires continued detailed exploration in vivo.

In conclusion, PQ-69 is one of the most potent and selective non-xanthine A_1AR antagonists yet described. The selectivity profile of PQ-69 for A_1AR vs $A_{2A}AR$ was 52-fold compared with 217-fold on human A_1R, and was superior to that of DPCPX. Moreover, PQ-69 displayed more potent inverse agonistic activity for A_1AR than DPCPX. We have demonstrated that PQ-69 has similar diuretic pharmacological properties to that of thiazide diuretics and DPCPX under normal conditions. Thus, PQ-69 represents a novel, potent and selective non-xanthine A_1AR antagonist with pronounced inverse agonist activity and in vivo bioactivity. This novel compound will be a useful tool to characterize physiological functions and complicated pathological conditions in relation to responses mediated by A_1ARs.

Acknowledgments These studies were supported by the National Science and Technology Major Projects "Major New Drugs Innovation and Development" (2009ZX09103-021) and Beijing Municipal Science & Technology Commission "Z121102002512046".

References

1. Fredholm BB, IJzerman AP (2011) International union of basic and clinical pharmacology. LXXXI. Nomenclature and classification of adenosine receptors—an update. Pharmacol Rev 63:1–34
2. Sebastião AM, Ribeiro JA (2009) Adenosine receptors and the central nervous system. Handb Exp Pharmacol 193:471–534

3. Chen JF, Eltzschig HK, Fredholm BB (2013) Adenosine receptors as drug targets—what are the challenges? Nat Rev Drug Discov 12: 265–286
4. Modlinger PS, Welch WJ (2003) Adenosine A_1 receptor antagonists and the kidney. Curr Opin Nephrol Hypertens 12:497–502
5. Schenone S, Brullo C, Musumeci F, Bruno O, Botta M (2010) A_1 receptors ligands: past, present and future trends. Curr Top Med Chem 10:878–901
6. Müller CE, Jacobson KA (2011) Recent developments in adenosine receptor ligands and their potential as novel drugs. Biochim Biophys Acta 1808:1290–1308
7. de Ligt RA, Kourounakis AP, IJzerman AP (2000) Inverse agonism at G protein-coupled receptors: (patho)physiological relevance and implications for drug discovery. Br J Pharmacol 130:1–12
8. Searl TJ, Silinsky EM (2012) Evidence for constitutively-active adenosine receptors at mammalian motor nerve endings. Eur J Pharmacol 685:38–41
9. He W, Wilder T, Cronstein BN (2013) Rolofylline, an adenosine A1 receptor antagonist, inhibits osteoclast differentiation as an inverse agonist. Br J Pharmacol 170:1167–1176
10. Liu CH, Wang B, Li WZ, Yun LH, Liu Y, Su RB, Li J, Liu H (2004) Design, synthesis, and biological evaluation of novel 4-alkylamino-1-hydroxyl-methylimidazo [1,2-a] quinoxalines as adenosine A_1 receptor antagonists. Bioorg Med Chem 12:4701–4707
11. von Bahr C, Groth CG, Jansson H, Lundgren G, Lind M, Glaumann H (1980) Drug metabolism in human liver in vitro: establishment of a human liver bank. Clin Pharmacol Ther 27: 711–725
12. Klotz KN, Hessling J, Hegler J, Owman C, Kull B, Fredholm BB, Lohse MJ (1998) Comparative pharmacology of human adenosine receptor subtypes—characterization of stably transfected receptors in CHO cells. Naunyn Schmiedebergs Arch Pharmacol 357:1–9
13. Cheng YC, Prusoff WH (1973) Mouse ascites sarcoma 180 thymidylate kinase. General properties, kinetic analysis, and inhibition studies. Biochemistry 12:2612–2619
14. Arunlakshana O, Schild HO (1959) Some quantitative uses of drug antagonists. Br J Pharmacol Chemother 14:48–58
15. Mandagere AK, Thompson TN, Hwang KK (2002) Graphical model for estimating oral bioavailability of drugs in humans and other species from their Caco-2 permeability and in vitro liver enzyme metabolic stability rates. J Med Chem 45:304–311
16. Zhuang XM, Deng JT, Li H, Kong WL, Ruan JX, Xie L (2011) Metabolism of novel anti-HIV agent 3-cyanomethyl-4-methyl-DCK by human liver microsomes and recombinant CYP enzymes. Acta Pharmacol Sin 32:1276–1284
17. Karasawa A, Kubo K, Shuto K, Oka T, Nakamizo N (1988) Antihypertensive effects of the new calcium antagonist benidipine hydrochloride in rats. Arzneimittelforschung 38:1684–1690